Clinical and Translational Radiation Oncology 51 (2025) 100904

Contents lists available at ScienceDirect

Clinical and Translational Radiation Oncology

journal homepage: www.sciencedirect.com/journal/clinical-and-translational-radiation-oncology

Original Research Article

Cardiorespiratory-gated cardiac proton radiotherapy using a novel ultrasound guidance system

Keith A Cengel [a,*], Zayne Belal [a], Michele M Kim [a], Sarah Hagan [a], Saskia Camps [b], Alexander Kalinin [b], Weihow Hsue [c], Eric Diffenderfer [a], Adriano Garonna [b], Cory Tschabrunn [c,d]

[a] Department of Radiation Oncology, University of Pennsylvania, Philadelphia, USA
[b] EBAMed SA, Geneva, Switzerland
[c] Smilow Center for Translational Research, Room 8-136, Univ of Pennsylvania, Perelman School of Medicine, 3400 Civic Center Blvd, Bldg 421, Philadelphia, PA 19104, USA
[d] Electrophysiology Section, Division of Cardiovascular Medicine, Hospital of the University of Pennsylvania, Philadelphia, PA, USA

ARTICLE INFO

Keywords:
Cardiac radiation
Gating
Ultrasound guidance

ABSTRACT

Cardiac stereotactic body radiotherapy is a promising noninvasive treatment for patients with refractory ventricular tachycardia. With the aim to prove feasibility of a novel image guided radiotherapy and heart motion gating device, cardiac proton radiotherapy was performed using a porcine model. Using a novel adaptation of γ – H2AX tissue staining techniques, we have been able to localize a radiation beam in large animal tissue to assess targeting accuracy within a defined field. Cardiorespiratory-gated irradiations of the animals were successfully completed and analysis of the γ-H2AX staining intensity of the excised heart after radiation demonstrated radiotherapy was delivered close to or within the expected region. We simulated the irradiated volumes under different gating scenarios, showing significant reduction when using combined cardiorespiratory gating. The results of this study show the feasibility of proton irradiation of the heart left ventricle with a novel ultrasound based cardiorespiratory gating technology with the benefit of reduced irradiation volumes and increased healthy tissue sparing.

Introduction

Standard clinical management of sustained monomorphic ventricular tachycardia (VT) in patients with Moreover, radiation dose to non-target heart structures by cardiac stereotactic body radiation therapy structural heart disease generally involves combinations of implantable cardioverter-defibrillator (ICD) placement, antiarrhythmic drugs, and catheter ablation [1]. While catheter ablation tools and techniques have steadily improved, creating effective and durable lesions remains a challenge, particularly when targeting intramural substrates in thick myocardium interspersed with fibrosis and fat [2]. Over the last 6 years, non-invasive cardiac stereotactic body radiation therapy has been proposed and increasingly utilized as an alternative treatment of cardiac arrhythmias, particularly in patients with recurrent ventricular arrhythmias despite aggressive treatment with antiarrhythmic drug therapy and catheter ablation procedures. While clinical benefit has been shown, the response has been variable in studies published to date [3–7]. The reasons for this variability remain incompletely understood, but one contributing factor could involve marginal missing of target substrate due to cardiorespiratory motion. Moreover, radiation dose to non-target heart structures by cardiac stereotactic body radiation therapy (SBRT) will likely lead to future adverse events events [8,9] and current techniques to account for cardiorespiratory motion result in the dramatic expansion of the target cardiac substrate volume in the final planning volume[10]. In this context, improved, dedicated image-guidance and gating could provide a valuable tool to both improve the accuracy of VT substrate targeting and increase healthy tissue sparing [11,12]. This would allow for potentially more consistent positive outcome, reduce the possible side effects of radiation on the non-target heart tissues and the surrounding organs at risk and increase the population eligible for cardiac radioablation. Moreover, as proton technologies expand to include novel and potentially highly motion sensitive

* Corresponding author.
E-mail address: keith.cengel@pennmedicine.upenn.edu (K.A. Cengel).

https://doi.org/10.1016/j.ctro.2024.100904
Received 9 December 2024; Accepted 18 December 2024
Available online 21 December 2024

techniques such as FLASH [13–15] and proton arc radiotherapy, the development of novel, real-time motion management take on an enhanced potential clinical significance for applications outside cardiac targeting.

Being non-invasive, safe and fast, ultrasound imaging is a natural candidate technology to address the specific challenges of real-time image-guidance for the heart, that are different from other applications in radiotherapy [16,17]. EBAMed SA is developing a novel image guided radiotherapy and heart motion gating device which in the rest of this work is referenced as CardioKit. Following first positive assessments of ultrasound image quality for ventricular tachycardia patients in supine position [18] and the impact of the probe position on the chest for proton and photon treatment plans [19], this study provides data on the feasibility of image-guided cardiorespiratory-gated cardiac proton radiotherapy on a porcine model. The verification of correct radiation delivery is based on γ-H2AX immunochemistry following procedures adapted from authors´ previous work on small animals [14,20]. These data serve as input for further CardioKit product development.

Materials and methods

Animal Preparation and Handling— Following approval by the University of Pennsylvania´s Institutional Animal Care & Use Committee, a total of three Yorkshire swine (referenced as "animal 1", "animal 2", "animal 3") underwent the study sequentially. Male subjects were chosen to minimize biological variabilities, given the insufficient statistical power to determine any sex-related impact on results and males more frequently develop scar-related Ventricular Tachycardia than females [21]. The body weight and age ranged from 57-60 kg and 3.5–4.5 months, respectively. After a quarantine period, surgical implantation of three to four 2 mm gold fiducial suture-type markers MTNW887866 (CQ Medical, USA) on the anterior lateral left ventricular wall. The surgery was performed under general anesthesia and the anatomical location was chosen to be representative of a ventricular tachycardia target.

Following recovery (3.5–4 weeks post-surgery) and overnight fasting, animals underwent simulation imaging and four days later, treatment. For simulation and treatment, the animals were sedated and medicated with beta-blockers. Regular respiration was ensured with a mechanical ventilator set to 18 cycles/min and 800 mL tidal volume. When, for imaging purposes, an expiratory breath-hold was required, this was reproducibly enforced by manually switching off the ventilator at end-exhale for a maximum of 30 s.

Simulation Imaging—All animals underwent data acquisition with CardioKit followed by Computed Tomography (CT) on a Siemens (Forchheim, Germany) Somatom Sensation Open using University of Pennsylvania's standard human clinical protocols as previously described [6]. Briefly, 4D contrast CT imaging was performed with 2 mm slice thickness with IV contrast given during the 4D scan that was respiratory-binned using a Varian RPM (Palo Alto, USA). In addition, a contrast-enhanced static CT was also acquired in expiratory breath-hold by briefly pausing the ventilator in end expiratory phase. Additionally, for animals 2 and 3, a 4D cardiac-binned contrast-enhanced CT was acquired using a Siemens (Forchheim, Germany) Somatom Force scanner. For all animals, transthoracic echocardiographic images were acquired in expiratory breath-hold prior to CT.

Treatment Planning —Treatment planning was performed using Eclipse treatment planning system (Varian, Palo Alto, CA) to deliver 25 Gy of stereotactic body radiation therapy with protons and was based on an end expiratory phase of the respiratory-binned 4D-CT (animals 1 and 3) or an expiratory breath hold CT (animal 2). The target was located at the center of the fiducial markers and consisted of 1–2 spots in 1–2 energy layers with a single beam direction perpendicular to the target tissue surface. For animals 1 and 2, a shoot-through method was used with a contralateral beam to create a sharp lateral penumbra at the location of the target. For animal 3, an ipsilateral beam with spread-out Bragg peak was used to more accurately represent a clinically planned treatment.

Treatment Delivery— Four days following simulation, the animals were aligned using Cone Beam Computed Tomography (CBCT) and irradiated with an Ion Beam Applications (Louvain-la-Neuve, Belgium) ProteusPlus therapy machine with gating signals provided by CardioKit (see next paragraph). As an initial test of the system, animal 1 was planned for treatment using only respiratory gating, whereas for animals 2 and 3, cardiorespiratory gating was used.

Cardiorespiratory gating — Cardiorespiratory gating was performed using a prototype of the novel ultrasound-based image guidance system (CardioKit) developed by EBAMed SA. It combines Electrocardiography (ECG), transthoracic echocardiography and optical tracking to enable real-time determination of the heart contraction state and heart displacement due to respiratory motion in the three spatial directions. The ECG module includes an online R-peak detection to determine the precise timing of ventricular contraction. The ultrasound probe images the heart at 50 Hz in two orthogonal planes and the spatial position of the probe is determined by optical tracking. Each ultrasound image is registered to a previously acquired reference ultrasound image to determine in real-time the displacement of the heart. Gating for cardiac motion is enabled by specifying an allowed motion interval in terms of % of the R-R interval, whereas gating for respiratory motion is enabled by specifying an allowed motion interval in terms of motion excursions from expiratory breath-hold in each spatial direction. The time delays linked to image and signal acquisition and real-time processing are precisely measured internally and taken into consideration for motion prediction. The information on the reaction times for beam generation/hold of the therapy machine is used to anticipate the generation of the gating commands, such that the beam is resumed/paused at the desired point in time.

Tissue Analysis—We have previously used staining for the DNA damage marker γ-H2AX in cardiac tissues to verify the accuracy of proton and photon beam delivery in mice [14,20]. To modify this method to be compatible with the considerably larger volumes in porcine heart tissues, we first divided the heart tissues into a 1–1.5 cm grid pattern using the implanted fiducials as a guide and then performed immunohistochemical analysis. Sections were frozen in Optimal Cutting Temperature (OCT Tissue-TEK) compound at the ~ 1 h post irradiation timepoint to maximize γ-H2AX signal intensity. Tissues were sectioned at 5 μm thickness and immunohistochemistry was performed using γ-H2AX with Hoechst nuclear counterstaining. Sections were fixed in 2 % paraformaldehyde, permeabilized in ice cold methanol, blocked with 8 % bovine serum albumen (BSA) in PBS with 0.5 % Tween-20 and 0.1 % Trition X-100 (PBS-TT) and incubated with Anti-phospho-Histone H2A. X (Ser139) Antibody (directly FITC-conjugated – Millipore, clone JBW301 – Ref 16-202A – diluted 1:500, in 1 % BSA in PBS-TT). Nuclei were counterstained with 5ug/ml Hoechst in PBS and imaged at 10x on a Zeiss Observer.Z1 inverted Fluorescent microscope with an AxioCam MRm camera (Zeiss). Once the beam signal was located, a control tissue section was selected from the sampled field at a distal location. Quantitative image analysis was performed using FIJI open source software. For each stained tissue section, signal intensity was calculated as the raw integrated density per γH2AX region of interest (ROI) divided by the total area of the corresponding Hoechst ROI for a minimum of 5 ROI per section. This was then plotted on a scale of 0 (negative) to 100 (maximum) signal intensity.

Results

Calibration of the optical tracker of the cardiorespiratory gating system (Fig. 1) was performed prior to simulation imaging and radiation delivery: the optical tracker was placed on the ceiling (or on a tripod when temporary placement on the ceiling was not possible) and a dedicated phantom with precisely placed optical and radio-opaque reference markers was used to determine the coordinate transformation between the tracker and the room coordinate system used for

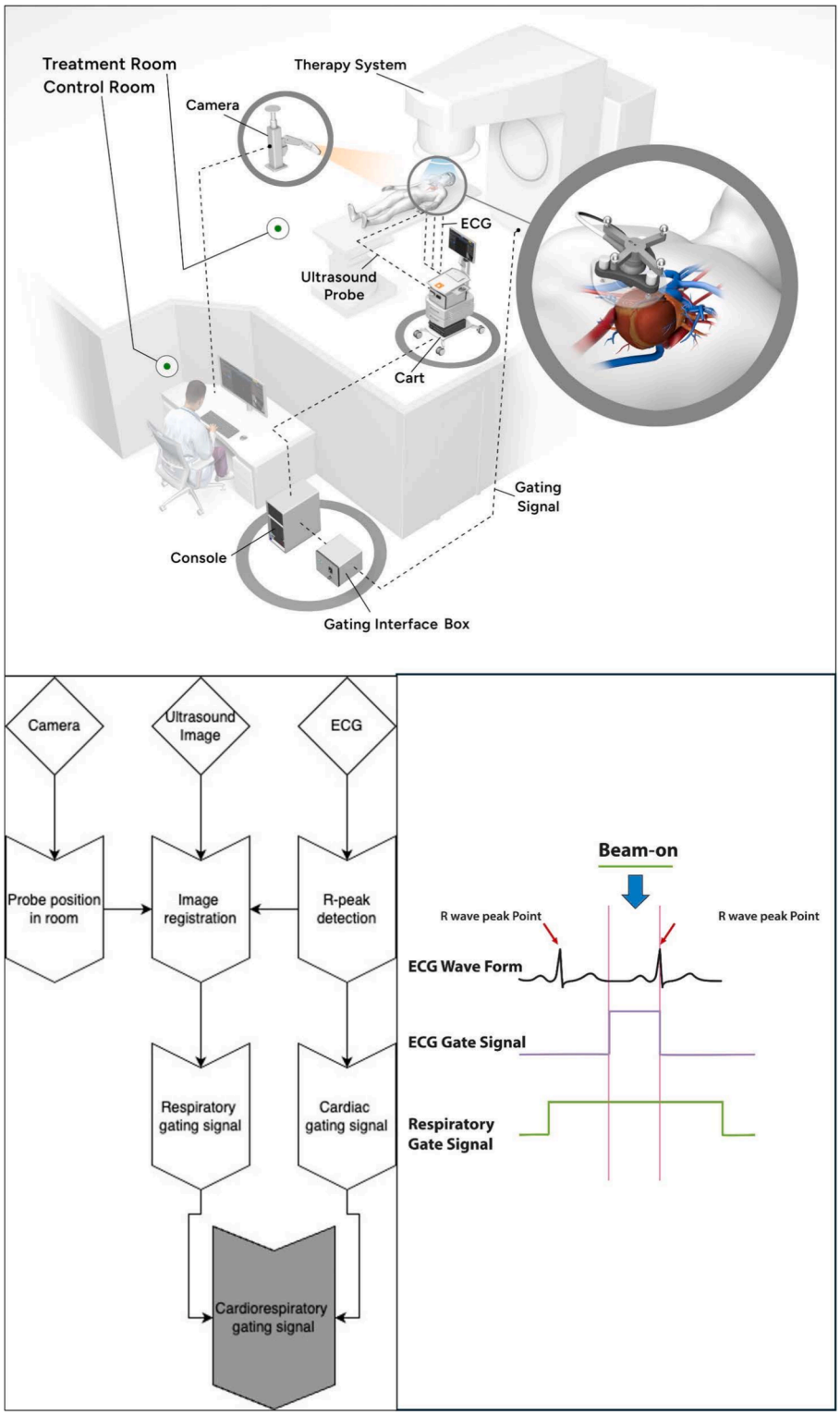

Fig. 1. Ultrasound based image guidance. (**Top**) Graphical representation of the ultrasound-guidance setup with CardioKit elements circled in gray and a zoom view of the ultrasound probe with optical markers fixed on the thorax with an adhesive patch. **(Bottom left)** Simplified diagram of the signal/image processing steps to generate a cardiorespiratory gating signal. **(Bottom right)** Schematic for gating using combination of ECG and respiratory motion signals.

simulation imaging and radiation delivery. The response time of the therapy machine to gating commands was characterized by measuring on a digital oscilloscope the time delays between the rising/falling edges of the input gating signal sent to the IBA gating interface and the output beam signal recorded on an ionization chamber placed at room isocenter.

The implanted fiducials on the left ventricle surface created a triangle of 3–3.5 cm per side, which was used to identify the target zone for treatment planning (Fig. 2**A**). For animal 1, a posterior beam was designed to target an ~ 1.5 cm area within this fiducial triangle (Fig. 2**B**)

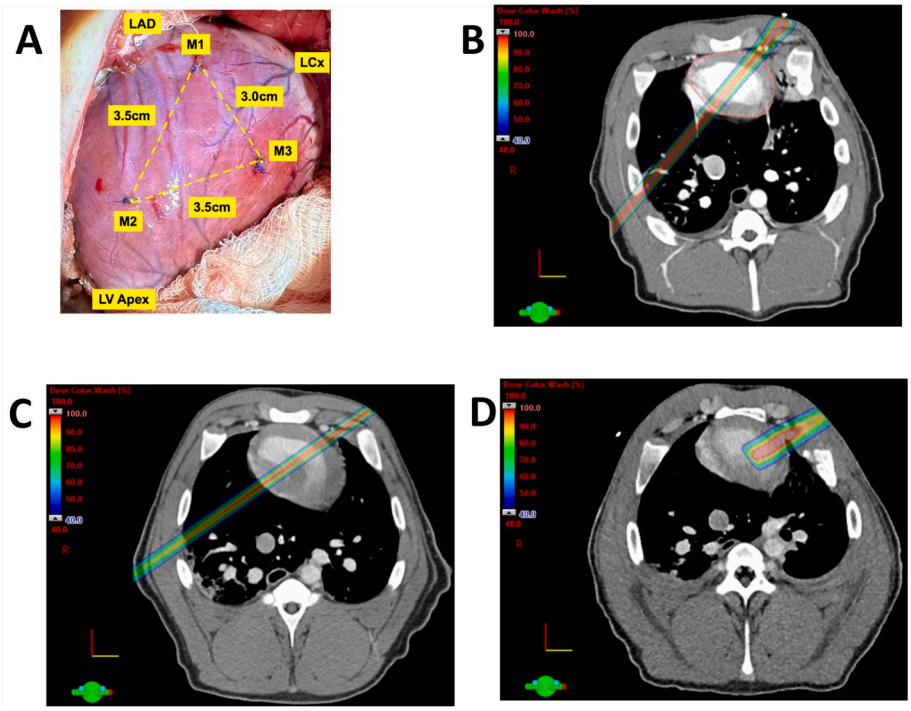

Fig. 2. Targeting and treatment planning. (**A**) For each animal, 3–4 fiducials were placed on the left ventricle surface. (**B,C**) treatment plan for animal 1 and 2 showing posterior beam targeting area within the fiducial triangle using a shoot through approach. (**C**) treatment plan for animal 3 showing anterior beam targeting area within the fiducial triangle using a pencil beam scanned spread out Bragg peak approach. Radiation doses are shown in color wash as indicated in top left of each panel.

using a shoot through technique. The respiratory gating windows were empirically adjusted to irradiate only in end expiration. The respiratory motion allowed in the gating window was 2 mm, 4 mm and 2 mm in the sagittal, axial and coronal directions, respectively. After irradiation and animal sacrifice, quantitative image analysis of γ-H2AX staining (see Fig. 3**A** for representative staining images). As shown in Fig. 3**B**, the targeted area from treatment planning (left panel) matches well with the quantitative image analysis for γ-H2AX staining (right panel), demonstrating excellent target localization using CardioKit respiratory targeting.

For Animal 2, in an attempt to simulate gated treatment only during the end expiratory respiratory phase, treatment planning was completed on an end expiratory breath hold CT, although both cardiac binned and respiratory binned CT series were also obtained to estimate cardiorespiratory motion parameters. Similarly to animal 1, a posterior shoot through proton beam plan was used (Fig. 2**C**). During treatment, the allowed respiratory motion in the gating window was 3 mm, 2 mm and 3 mm in the sagittal, axial and coronal directions, respectively. The cardiac gating window was defined as the interval between the end of the T-wave and the start of the P-wave in the ECG signal (45–80 % R-R interval), which corresponds to the end of the filling phase of the heart. This interval was chosen to increase the possibility to spare healthy myocardium and critical cardiac structures. Analysis of the targeting by γ-H2AX staining demonstrates that the area treated was more apical-laterally located that the area that was targeted (Fig. 4**A**). Further analysis comparing the 4D respiratory CT end expiratory phase to the expiratory breath hold CT suggested that the position/angle of the heart is different on these two scans, possibly due to differences in cardiac filling induced by breath hold.

To account for these differences, animal 3 irradiation was planned using the end expiratory phase of the respiratory binned CT. Moreover, to better simulate an actual patient treatment with proton beam radiotherapy, the treatment area was planned using a ~ 1.5 cm target treated with an anterior beam and a pencil beam scanned, spread out Bragg

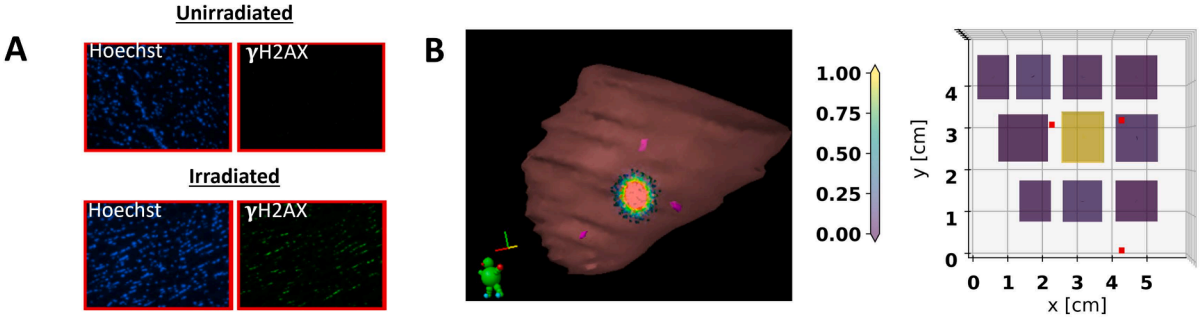

Fig. 3. Analysis of γ-H2AX staining with respiratory gated delivery. (**A**) Representative images of staining from non-targeted (top) vs targeted (bottom) areas of heart (**B**) 3 dimensional representations of the planned target area (left panel) vs plot of γ-H2AX staining intensity (right panel) of heart sections near the fiducial markers (demonstrated as red dots) for animal 1. For (B), each heart tissue section is represented by a rectangle with lateral dimensions along x and y directions corresponding to the position measured on the dissection board and color proportional to the relative γ-H2AX staining intensity.

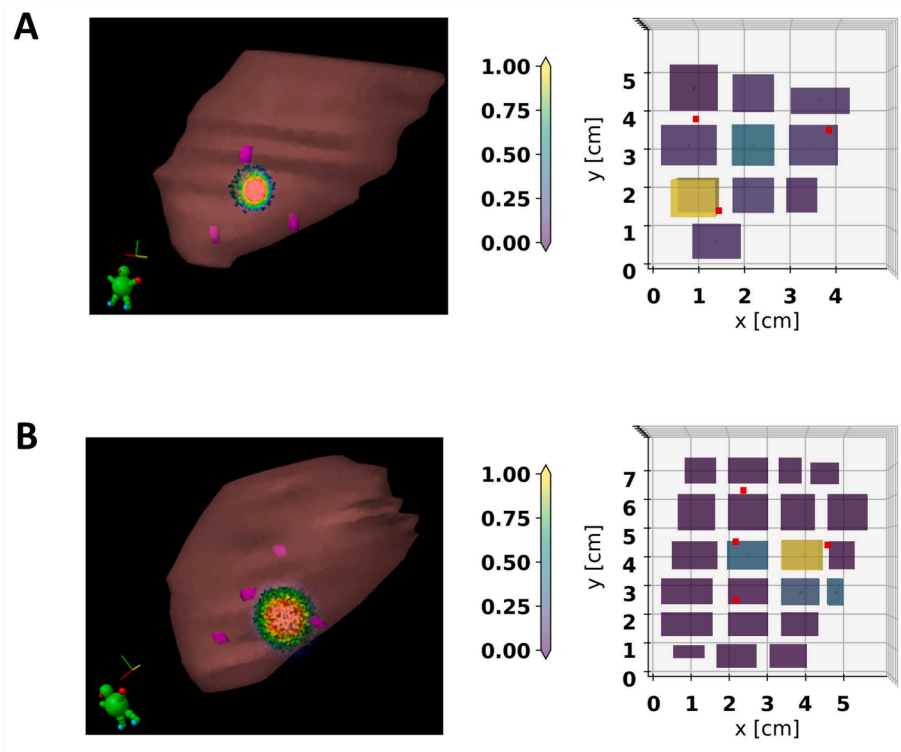

Fig. 4. Analysis of γ-H2AX staining for cardiorespiratory gated delivery. 3 dimensional representations of the planned target area (left panel) vs plot of γ-H2AX staining intensity (right panel) of heart sections near the fiducial markers (demonstrated as red dots) for animal 2 (**A**) and animal 3 (**B**). For (B), each heart tissue section is represented by a rectangle with lateral dimensions along x and y directions corresponding to the position measured on the dissection board and color proportional to the relative γ-H2AX staining intensity.

peak approach (Fig. 2 **D**). During treatment, the allowed respiratory motion in the gating window was 4 mm, 5 mm and 5 mm in the sagittal, axial and coronal directions. To maximize target size homogeneity and spare maximum healthy tissues, the left ventricular volume on the cardiac gated CT was analyzed to determine when the heart would be between 80–100 % of its end diastolic volume. Based on this, the gating window was set to 60–99 % of R-R interval. Analysis of the cardiac tissues by γ-H2AX staining demonstrates excellent correspondence between the planned and actual irradiated tissues (Fig. 4**B**), thus showing that the CardioKit can provide accurate gated treatment of cardiac tissues using a clinically relevant treatment plan.

Gated irradiation of the animals was successfully completed with an average total irradiation time of 4 min. No extra systole or other arrhythmic event was recorded during the procedures. The heartbeat varied between 60 beats per minute (BPM) and 105 BPM, with for each animal variations of max 15 BPM during simulation and 10 BPM during treatment. The maximum difference between heart rates between simulation and treatment was 10 BPM.

The goal of obtaining a small, irradiated area with the sharpest possible lateral dose fall-off resulted in treatment plans which are not representative of ventricular tachycardia treatment plans. In order to provide a more accurate representation of the potential clinical benefit of gating, we analyzed the motion of the left ventricle free wall. To estimate the potential changes in treatment volume that might be obtained with cardiorespiratory gating, a target area on the inferolateral wall was identified on all cardiac and respiratory phases of CTs for animals 2 and 3 using cardiac landmarks including papillary muscle insertions as a guide for contouring. The gross target volume (GTV) for each animal was the volume of ventricle wall on either the CT average scan ("ungated" scenarios) or the end expiratory phase of the scan ("gated" scenarios). For the ungated analyses, the internal target volume (ITV) was the sum of the target volumes on respiratory or cardiac gated phases for each animal. For the gated analyses, the respiratory ITV was created using the residual motion recorded by the CardioKit system and the cardiac ITV was created by summing the cardiac target volumes only from the gated cardiac phases. This analysis demonstrates a 23–37 % saving of ITV volume for gated as compared to ungated treatments (Table 1).

Discussion

The study shows that proton irradiation of the heart left ventricle with a novel ultrasound-based cardiorespiratory system was feasible in all 3 healthy swine. Irradiation times were clinically acceptable and the workflow for calibration, configuration and operation of the system was viable. The small sample size does not allow to make a statistical assessment of the findings but does provide solid proof-of-concept data. The limitations of the study are linked to: the use of sedated animals under controlled ventilation (with enforced breath-holds), the idealized target locations due to the absence of a clinical target in the healthy myocardium and the simple treatment plans with a single beam direction.

The determination of the effective radiation delivery using γ-H2AX that we and others have used in previous small animal work was found to be applicable also for the larger volume of the heart of swine. The imaging post-treatment showed delivery of the radiation at the expected area for two animals and close to the expected area for one animal. This radiation delivery confirmation method allows to provide a rapid assessment, compared to other animal imaging studies involving radiation to the heart [22]. We note that even with our analysis methods, quantitative assessment of the accuracy of the ultrasound-based motion management system on a millimetric scale would be challenging given the inherent difficulties processing large animal tissues for later pathologic evaluation.

The simulation work presented in this study comparing the irradiation volumes for a target in the left ventricle of two animals under

Table 1
Analysis of potential target volume sparing achieved by gating. Volume comparisons of: static target (contoured on 70% R-R phase of contrast-enhanced cardiac-binned 4D-CT), internal target volume including target expansions linked to cardiac contraction (based on contrast-enhanced cardiac-binned 4D-CT), respiratory motion (based on respiratory-binned 4D-CT) and the combination of both.

	Animal 2			Animal 3		
Volume in mL	Ungated	Gated	% Change	Ungated	Gated	% Change
Target	22.6	20.8	− 8.0	26.9	22.6	− 16.0
ITV_Cardiac	61.4	33.4	− 45.6	73.5	42.6	− 42.0
ITV_Respiratory	44.7	31.9	− 28.6	57.4	46	− 19.9
ITV_Cardiorespiratory	63	39.5	− 37.3	77.3	59.5	− 23.0

different gating scenarios demonstrates the benefit of gating in significantly reducing the target volume expansions required for motion management, opening the way to potentially safer treatments. However, the related increased sparing of healthy tissues could not be demonstrated in this acute study and will need to be assessed in further work with a long post-irradiation follow-up to record the possible occurrence of any side-effects. It should also be noted that the volumetric comparisons may not be representative of the situation for STAR patients with large scarred ventricular myocardium and thus reduced contractility. Indeed, the target in this animal study is in a healthy myocardium, the mediastinum of pigs is different compared to humans and adhesions between the heart and the chest wall linked to the surgical procedure of metal clip implantation could have reduced the amplitude of heart motion linked to respiratory motion.

Finally, the results of this study also suggest that changes in reproducibility in cardiac anatomy between breath holding and free breathing CT averaged based targeting could present unique challenges that merit further analysis and consideration going forward. Further work could focus on proving the feasibility of ultrasound-based image guidance for FLASH irradiations.

CRediT authorship contribution statement

Keith A Cengel: Methodology, Software, Validation, Formal analysis, Investigation, Writing – review & editing, Supervision, Funding acquisition. **Zayne Belal:** Validation, Formal analysis, Writing – review & editing. **Michele M Kim:** Methodology, Validation, Formal analysis, Investigation, Writing – review & editing. **Sarah Hagan:** Methodology, Validation, Formal analysis, Investigation, Writing – review & editing. **Saskia Camps:** Methodology, Software, Validation, Investigation, Writing – review & editing. **Alexander Kalinin:** Methodology, Software, Validation, Investigation, Writing – review & editing. **Weihow Hsue:** Methodology, Validation, Formal analysis, Investigation, Writing – review & editing. **Eric Diffenderfer:** Methodology, Validation, Formal analysis, Investigation, Writing – review & editing. **Adriano Garonna:** Methodology, Software, Formal analysis, Investigation, Writing – review & editing, Supervision, Funding acquisition. **Cory Tschabrunn:** Methodology, Validation, Formal analysis, Investigation, Writing – review & editing, Supervision, Funding acquisition.

Declaration of competing interest

The authors declare the following financial interests/personal relationships which may be considered as potential competing interests: Collaborative Research Agreement between the University of Pennsylvania and EBAMed SA (Switzerland).

Acknowledgments

The authors wish to acknowledge the support from Beryl Bell, Francois Vander Stappen and their colleagues from Ion Beam Applications SA for the tests to characterize the response times to gating commands of the University of Pennsylvania ProteusPlus system. This work was funded by a collaborative research agreement between investigators at the University of Pennsylvania and EBAMed, SA and is part of a project that has received funding from the European Union's Horizon 2020 research and innovation program under grant agreement No 954783.

References

[1] Cronin EM, Bogun FM, Maury P, Peichl P, Chen M, Namboodiri N, et al. 2019 HRS/EHRA/APHRS/LAHRS expert consensus statement on catheter ablation of ventricular arrhythmias. Heart Rhythm 2020;17(1):e2–154.
[2] Barkagan M, Leshem E, Shapira-Daniels A, Sroubek J, Buxton AE, Saffitz JE, et al. Histopathological characterization of radiofrequency ablation in ventricular scar tissue. JACC Clin Electrophysiol 2019;5(8):920–31.
[3] Neuwirth R, Cvek J, Knybel L, Jiravsky O, Molenda L, Kodaj M, et al. Stereotactic radiosurgery for ablation of ventricular tachycardia. Europace 2019;21(7):1088–95.
[4] Zhang DM, Navara R, Yin T, Szymanski J, Goldsztejn U, Kenkel C, et al. Cardiac radiotherapy induces electrical conduction reprogramming in the absence of transmural fibrosis. Nat Commun 2021;12(1):5558.
[5] Robinson CG, Samson PP, Moore KMS, Hugo GD, Knutson N, Mutic S, et al. Phase I/II trial of electrophysiology-guided noninvasive cardiac radioablation for ventricular tachycardia. Circulation 2019;139(3):313–21.
[6] Arkles J, Markman T, Trevillian R, Yegya-Raman N, Garg L, Nazarian S, et al. One-year outcomes after stereotactic body radiotherapy for refractory ventricular tachycardia. Heart Rhythm 2024;21(1):18–24.
[7] Miszczyk M, Hoeksema WF, Kuna K, Blamek S, Cuculich PS, Grehn M, et al. Stereotactic arrhythmia radioablation (STAR)-A systematic review and meta-analysis of prospective trials on behalf of the STOPSTORM.eu consortium. Heart Rhythm 2024.
[8] Natarajan J, Yegya-Raman N, Kegelman TP, Kallan MJ, Roshkovan L, Katz S, et al. Cardiovascular substructure dose and cardiac events following proton- and photon-based chemoradiotherapy for non-small cell lung cancer. Adv Radiat Oncol 2023;8(5):101235.
[9] Yegya-Raman N, Ho Lee S, Friedes C, Wang X, Iocolano M, Kegelman TP, et al. Cardiac radiation dose is associated with inferior survival but not cardiac events in patients with locally advanced non-small cell lung cancer in the era of immune checkpoint inhibitor consolidation. Radiother Oncol 2024;190:110005.
[10] Stevens RRF, Hazelaar C, Fast MF, Mandija S, Grehn M, Cvek J, et al. Stereotactic arrhythmia radioablation (STAR): assessment of cardiac and respiratory heart motion in ventricular tachycardia patients - a STOPSTORM.eu consortium review. Radiother Oncol 2023;188:109844.
[11] Lee H, Pursley J, Lu HM, Adams J, DeLaney T, Chen YL, et al. A proof of concept treatment planning study of gated proton radiotherapy for cardiac soft tissue sarcoma. Phys Imaging Radiat Oncol 2021;19:78–84.
[12] Hohmann S, Deisher AJ, Suzuki A, Konishi H, Rettmann ME, Merrell KW, et al. Left ventricular function after noninvasive cardiac ablation using proton beam therapy in a porcine model. Heart Rhythm 2019;16(11):1710–9.
[13] Diffenderfer ES, Sorensen BS, Mazal A, Carlson DJ. The current status of preclinical proton FLASH radiation and future directions. Med Phys 2022;49(3):2039–54.
[14] Kim K, Kim MM, Skoufos G, Diffenderfer ES, Motlagh SAO, Kokkorakis M, et al. FLASH proton radiation therapy mitigates inflammatory and fibrotic pathways and preserves cardiac function in a preclinical mouse model of radiation-induced heart disease. Int J Radiat Oncol Biol Phys 2024;119(4):1234–47.
[15] Kim MM, Zou W. Ultra-high dose rate FLASH radiation therapy for cancer. Med Phys 2023;50(Suppl 1):58–61.
[16] Fontanarosa D, van der Meer S, Bamber J, Harris E, O'Shea T, Verhaegen F. Review of ultrasound image guidance in external beam radiotherapy: I. treatment planning and inter-fraction motion management. Phys Med Biol 2015;60(3):R77–.
[17] O'Shea T, Bamber J, Fontanarosa D, van der Meer S, Verhaegen F, Harris E. Review of ultrasound image guidance in external beam radiotherapy part II: intra-fraction motion management and novel applications. Phys Med Biol 2016;61(8):R90–.
[18] Casula M, Dusi V, Camps S, Gringet J, Benoit T, Garonna A, et al. Feasibility of an automatic ultrasonographic image acquisition system associated with an artificial intelligence algorithm for real-time monitoring of cardiac motion during cardiac radio-ablation. Front Cardiovasc Med 2022;9:849234.
[19] Perrin R, Maguire P, Garonna A, Weidlich G, Bulling S, Fargier-Voiron M, et al. Case report: treatment planning study to demonstrate feasibility of transthoracic ultrasound guidance to facilitate ventricular tachycardia ablation with protons. Front Cardiovasc Med 2022;9:849247.

[20] Dreyfuss AD, Goia D, Shoniyozov K, Shewale SV, Velalopoulou A, Mazzoni S, et al. A novel mouse model of radiation-induced cardiac injury reveals biological and radiological biomarkers of cardiac dysfunction with potential clinical relevance. Clin Cancer Res 2021;27(8):2266–76.
[21] Tschabrunn CM, Roujol S, Nezafat R, Faulkner-Jones B, Buxton AE, Josephson ME, et al. A swine model of infarct-related reentrant ventricular tachycardia: electroanatomic, magnetic resonance, and histopathological characterization. Heart Rhythm 2016;13(1):262–73.
[22] Imamura K, Deisher AJ, Dickow J, Rettmann ME, Yasin OZ, Pepin MD, et al. Early impact of proton beam therapy on electrophysiological characteristics in a porcine model. Circ Arrhythm Electrophysiol 2023;16(6):e011179.